

# Experimental Evaluation of Intrinsic and Nonstationary Ultrasonic Doppler Spectral Broadening in Steady and Pulsatile Flow Loop Models

Guy Cloutier, *Member, IEEE*, K. Kirk Shung, *Fellow, IEEE*, and Louis-Gilles Durand, *Senior Member, IEEE*

**Abstract**—Intrinsic and nonstationary Doppler spectral broadening, and the skewness of the spectral representation, were evaluated experimentally using porcine red cell suspensions as ultrasonic scatterers. Intrinsic broadening, by definition, refers to the broadening produced by the range of angles sustained by each scatterer viewed by the finite dimension of the transducer. Nonstationary broadening refers, on the other hand, to the broadening associated with the acceleration and deceleration of the scatterers within the Doppler sample volume. Theoretically, the relative Doppler bandwidth, defined as the intrinsic bandwidth divided by the mean Doppler frequency shift, should be velocity independent. In the present study, the relative Doppler bandwidth invariance theorem was experimentally verified with an *in vitro* steady laminar blood flow model. We showed that the relative bandwidth was both independent of the flow velocity and blood hematocrit. Using a pulsatile laminar flow model, we demonstrated that the relative Doppler bandwidth invariance theorem did not hold during flow acceleration and deceleration. In addition, a positive skewness of the Doppler spectra was observed during acceleration while a negative skewness was measured during the deceleration of blood. The effect of the window duration used in the Fourier spectral computation, on nonstationary broadening, was also characterized. For a window of 2.5 ms, broadening due to spectral leakage dominated over nonstationary broadening. The limitation of the spectrum analyzer was less important for windows of 5 and 10 ms. Experiments were also performed in pulsatile turbulent flow to verify the behavior of the relative Doppler bandwidth and spectral skewness. In this flow regime, both parameters significantly varied within the flow cycle, with a pattern of variation different from that observed in pulsatile laminar flow. Generally, good matching was found between experimental and theoretical results. Significant basic information on the backscattering of ultrasound from blood in both steady and pulsatile flow is presented in this study.

## I. INTRODUCTION

Manuscript received January 27, 1993; revised May 4, 1993; accepted May 4, 1993. This work was supported by a postdoctoral research fellowship from the Natural Sciences and Engineering Research Council of Canada and by a research scholarship from the Fonds de la Recherche en Santé du Québec to Dr. Cloutier, and by the National Institutes of Health under NIH Grant HL28452.

G. Cloutier and L.-G. Durand are with the Laboratoire de génie biomédical, Institut de recherches cliniques de Montréal, 110 avenue des Pins Ouest, Montréal, Québec, Canada, H2W 1R7.

K. K. Shung is with the Bioengineering Program, The Pennsylvania State University, 233 Hallowell Building, University Park, Pennsylvania, U.S.A., 16802.

IEEE Log Number 9211578.

### A. Intrinsic Spectral Broadening

“INTRINSIC Doppler spectral broadening,” which is now a commonly used terminology [1], refers to the broadening due to the properties of the measurement system rather than the nature of the flow. In addition to the phenomenon of intrinsic spectral broadening, the velocity distribution within the sample volume (e.g., flat or parabolic), the flow characteristics (e.g., laminar or turbulent), the nonstationarity of the signal, and the properties of the spectrum analyzer are other factors contributing to the width of the Doppler spectrum. Some of these factors were studied theoretically or experimentally while information is lacking on others.

The phenomenon of intrinsic spectral broadening has been studied for many years in order to better understand the properties of the backscattered Doppler signals, and also for achieving the objective of improving the diagnosis of minimal flow disturbances by minimizing its effect. Extensive theoretical analyses on intrinsic broadening were performed by Newhouse *et al.* [2]–[4]. A theory describing the broadening produced by the transit-time of the ultrasonic scatterers within the continuous-wave (CW) acoustic beam, and the resulting amplitude modulation of the Doppler signal was described in [2]. Later, a geometrical approach, equivalent to the transit-time theory [4], was used to characterize Doppler spectral broadening [3], [5]. The generalization of the theory for both CW and pulsed-wave (PW) ultrasonic Doppler can be found in a paper by Censor *et al.* [6]. In this numerical theoretical model, PW ultrasonic excitation with many pulses and a steady laminar flow were assumed. Moreover, the particles producing the Doppler spectrum were presumed uncorrelated which is known to be invalid for blood flow at normal hematocrit [7]. For constant flow (flat velocity profile) crossing the focal area of a focused circular transducer, the intrinsic PW Doppler spectral bandwidth was given by [6], [8]:

$$B_d = \frac{2\nu W \sin \theta}{\lambda F}, \quad (1)$$

where  $\nu$  is the flow velocity of the moving target,  $W$  the diameter of the transducer,  $\theta$  the angle between the velocity vector and the ultrasonic beam,  $\lambda$  the wavelength of the ultrasonic signal, and  $F$  the focal length of the transducer. By combining (1) with the general Doppler shift equation (see

[1]), the intrinsic PW Doppler spectral broadening can also be expressed as:

$$B_d = \frac{f_d W \tan \theta}{F}, \quad (2)$$

where  $f_d$  represents the Doppler frequency shift of the moving target.

By looking at (2), it can be observed that the relative Doppler bandwidth  $B_d/f_d$  is theoretically velocity independent. This postulate was verified experimentally by Tortoli *et al.* [9] using a string target as Doppler scatterer. As predicted by the theoretical study by Newhouse and Reid [8], Tortoli *et al.* [9] verified experimentally that changes in the range (depth of measurement) and lateral displacement of the transducer had no significant effect on the relative Doppler bandwidth. In the study by Tortoli *et al.* [9], two PW Doppler transducers having different beam patterns and operating at 4 and 5 MHz were used to test the relative bandwidth invariance theorem. In that study, changes in the length of the PW sample volume were shown to have no effect on the relative Doppler bandwidth.

### B. Nonstationary Broadening

Very few studies have addressed the problem of the influence of time-varying flow on the Doppler signal. This issue was briefly addressed by Censor *et al.* [6] who showed that the shape of the spectrum should theoretically skew in unsteady flow. In another theoretical study [10], the same problem was also addressed and it was demonstrated that the backscattered signal, produced by a single scattering particle passing through the ultrasound beam, is transformed as a wide-band frequency modulated (FM) signal with  $v(t)$ , the time-varying velocity of the target, being the modulating parameter in nonstationary flow. In addition to the influence of time-varying velocity, another parameter is important in describing the spectral broadening in presence of unsteady flow. This parameter, addressed by Fish [11], is the length of the data window used to compute the Doppler Fourier spectrum. In practice, the Doppler signal due to blood flow is generally considered stationary over a data window of approximately 10 ms. During physiological flow acceleration and deceleration, nonstationary broadening might be present over such a data window. A compromise has then to be reached [11] because, on one hand, a small window duration increases the measured Doppler bandwidth, due to the reduction of the resolution of the spectral algorithm (spectral leakage), and on the other hand, such small window duration reduces nonstationary broadening associated with the variation of velocity in the data window.

### C. Objectives

In the present study, the spectral broadening in presence of steady laminar parabolic flow, pulsatile laminar flow, and pulsatile turbulent flow was experimentally quantified. To the best of our knowledge, no result currently exists on experimental validation of the relative Doppler bandwidth invariance theorem with blood as ultrasonic scatterer. Moreover, no experimental study has been performed to examine the effect of pulsatile flow on the Doppler bandwidth.

The general objectives of the present study were: 1) to validate experimentally, using a blood flow loop model, the relative Doppler bandwidth invariance theorem, 2) to show that nonstationary broadening exists for simulated blood flow velocity versus time traces similar to that found in normal human femoral arteries, 3) to show that the shape of the Doppler spectrum is skewed in pulsatile flow, and 4) to evaluate the effect of turbulence on the relative Doppler bandwidth and spectral skewness in pulsatile flow. A secondary objective was to demonstrate that the Doppler bandwidth invariance theorem was still valid for correlated scatterers (i.e., for blood at normal hematocrit).

## II. MATERIALS AND METHODS

Fresh porcine blood was used in this research. A solution of 1 g of ethylenediamine tetra-acetic acid (EDTA) in 10 ml of saline was added to whole blood at a concentration of 30 ml per liter of blood to prevent coagulation. To avoid crenation of the red cells, bovine albumin was added to the suspended erythrocytes at a concentration of 0.5 g per 100 ml. Concentrated erythrocytes were first obtained by centrifuging the whole blood and removing the plasma and the top white cell layer. The red cells were then washed twice with 0.9% saline buffered to pH 7.4, and centrifugation was used at each step to separate the erythrocytes from the saline solution. When reconstituting blood to desired hematocrits by mixing red cells with isotonic saline solution, the concentration of red cells was assessed by microcentrifugation.

Both steady and pulsatile flow loop arrangements were used. A complete description of the flow models can be found in [12], [13]. A brief summary of the experimental arrangement, technical specification of the Doppler ultrasonic system, and digital processing of the signals is given in this section.

The main flow conduit immersed horizontally in a water tank to allow acoustic coupling was a cylindrical Tygon tube for steady flow experiments, and a high pressure polyethylene tube for pulsatile flow experiments. Both flow conduits had an inner diameter of 0.476 cm. To allow for a better sound transmission, an acoustic window was cut in the Tygon tube at the site of Doppler recordings. For the steady flow model, the flow rate in the main conduit was gravity driven and was controlled by adjusting the height difference between two reservoirs, one located at the entrance of the main conduit and another positioned at its exit. A calibrated roller pump with variable speed was used to recirculate blood from the exit reservoir to the entrance reservoir thereby preserving the height difference between the blood levels. Based on fluid dynamics consideration [12], it was assumed that fully developed laminar flow was present at the location of insonation. Mean flow velocities within the tube of 10, 25, 30, 40, and 55 cm/s were used in steady flow experiments.

In nonstationary flow experiments, a Harvard pulsatile pump (model 1423) was used to simulate physiological pulsatile flow waveforms. Flow profiles similar to that found in normal human femoral arteries were simulated [13]. For both steady and pulsatile flow configurations, an electromagnetic flowmeter (Carolina Medical Electronics, model 501) was used

along with a blood flow probe (In Vivo Metric, model *K*) to monitor the instantaneous mean flow rate within the tube. The pump and tube arrangements were adjusted to obtain a mean flow velocity within the tube of 11 cm/s and a maximal flow velocity at peak systole of approximately 60 cm/s, as measured with the electromagnetic flowmeter.

A pulsed Doppler flowmeter developed by Hartley [14] was used to transmit and receive Doppler signals. The angle between the tube and the Doppler probe was maintained at 60 degrees for steady flow experiments, and 70 degrees in pulsatile flow. The width and length of the PW sample volume were determined experimentally using the following approach. The  $-3$  and  $-6$  dB beam widths were evaluated by using the pulse-Doppler probe as a pulse-echo A-mode probe. The transducer was then fired with bursts of 10 MHz ultrasound signals and the transmitted amplitude was detected in  $x$ ,  $y$ , and  $z$  directions with a NP-1000 needle hydrophone (NTR Systems, model TNU001A) mounted on a three-dimensional step motor arrangement. The average diameters of the beam width, 1.5 cm from the face of the transducer, were 1.05 mm ( $-3$  dB) and 1.52 mm ( $-6$  dB). The length of the sample volume was 0.55 mm as computed with the following equation [1]:

$$Z_r = \frac{c(t_g + t_p)}{2} \quad (3)$$

where  $c$  is the speed of ultrasound in blood (1570 m/s),  $t_g$  the duration of the gated returned ultrasonic signals (0.3  $\mu$ s), and  $t_p$  the duration of the transmitted ultrasonic bursts (0.4  $\mu$ s). The three-dimensional size of the sample volume ranged between 0.5 ( $-3$  dB) and 1.0 mm<sup>3</sup> ( $-6$  dB) depending of the definition used to estimate the beam width.

All Doppler measurements were performed by positioning the sample volume at the center of the main flow conduit, 1.5 cm from the face of the transducer. Measurements were obtained from the beginning of the far field zone of the transducer, where the beam width was minimal. The ultrasonic beam at the site of measurement was axially symmetrical and cylindrical. The beam divergence was minimal over the length of the sample volume. The pulsed Doppler flowmeter was operated with a nonfocused 10 MHz transducer having a diameter of 0.3 cm. A small focusing effect was experimentally detected since the beam width was smaller than the transducer aperture for the range selected. The pulse repetition frequency was 20 and 40 kHz in steady and pulsatile flow, respectively.

The forward signal of the PW Doppler system and the flow rate signal from the electromagnetic flowmeter were digitized by a Hewlett-Packard (HP) digitizing scope (model 54501A) to 8 bits at a rate of 25.6 kHz in steady flow, and 51.2 kHz in pulsatile flow. Acquisition of the Doppler signals at different moments within flow acceleration and deceleration was realized by triggering the flow rate signal and adjusting the delay of the HP oscilloscope. An IEEE-488 interface board was used to transfer the digitized data to a personal computer. The digitized signal was then windowed with a 10-ms Hanning function, zero padded to 1024 samples, fast Fourier transformed, and squared to obtain a power spectral representation of the Doppler signal. Power spectra using data

windows of 5 and 2.5 ms were also computed. The spectral resolution (bandwidth of a pure sine wave) of the spectrum using the Hanning function and the Fourier transform is  $4/T$  [15], where  $T$  is the duration of the data window in second. For windows of 10, 5, and 2.5 ms, the spectrum resolutions associated with the main lobe width are 400, 800, and 1600 Hz, respectively. This broadening due to the properties of the spectrum analyzer is independent of the flow velocity, flow characteristics, and properties of the Doppler instrument. In steady flow, mean Doppler power spectra were obtained by averaging 500 spectra while averaging over 200 cycles was used in pulsatile flow.

With the pulsatile flow arrangement, turbulence was generated in some experiments by introducing a mesh screen in the main flow conduit, 2 cm upstream of the Doppler measurement site. The mesh was removed for laminar flow measurements. The mesh was made of perpendicular round bars of 0.023-cm diameter, and a wire spacing of 0.106 cm was used.

#### A. Computation of the Relative Doppler Bandwidth

For each Doppler mean spectrum, its minimal and maximal frequencies were first extracted by computing the bandwidth at  $-10$  dB below the maximal power of the spectrum. Within the bandpass of the resulting spectrum, the first (mean), second (variance), and third moments were computed and used to evaluate the relative Doppler bandwidth, and to quantify the skewness of the spectral representation. Such a high threshold was used to ensure that no spectral noise component was present in the computation of the statistical moments.

The coefficient of variation (*CV*) was used to estimate the relative Doppler bandwidth. *CV* was first computed for each mean spectrum using the following equation:

$$CV = \left| \frac{\sqrt{m_2}}{m_1} \right| = \left| \frac{\sigma}{\mu} \right|, \quad (4)$$

where  $m_1$  is the first moment,  $m_2$  the second moment,  $\mu$  the statistical mean, and  $\sigma$  the standard deviation calculated from the mean spectra. Assuming that the shape of the Doppler spectra follows that of a Gaussian statistical distribution in steady flow, we can postulate that 99.7% of the spectral energy is contained within  $f_d \pm 3\sigma$ . From this postulate, the Doppler bandwidth was estimated as being equal to  $6\sigma$ . Consequently, the following equation was used to estimate the relative Doppler bandwidth  $B_d/f_d$  theoretically defined in (2):

$$B_d/f_d \approx \left| \frac{6\sigma}{\mu} \right| = 6 \times CV \quad (5)$$

#### B. Evaluation of the Skewness of Doppler Mean Spectra

The degree of skewness of Doppler mean spectra was assessed by computing the following equation:

$$\alpha_3 = \frac{m_3}{\sigma^3}, \quad (6)$$

where  $m_3$  is the statistical third moment. Fig. 1 provides a visual interpretation of the coefficient of skewness  $\alpha_3$ .

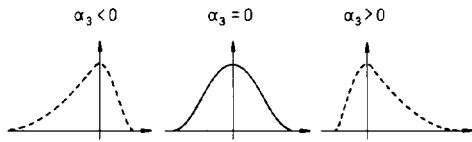


Fig. 1. Visual interpretation of the coefficient of skewness  $\alpha_3$ . A coefficient value of 0 corresponds to a symmetrical distribution while values lower or greater than 0 correspond to a negatively or positively skewed distribution.

C. Statistical Analyses

All results presented next are expressed in term of mean  $\pm$  standard deviation. One-way analyses of variance (ANOVA) with repeated measurements were computed to assess possible dependence of the relative Doppler bandwidth and coefficient of skewness on variations in blood hematocrits, steady flow velocities, and positions within the pulsatile flow period. A statistical significance level of 0.01 was used as decision threshold. Unpaired *T*-test was also used to compare mean values of the relative Doppler bandwidth.

III. RESULTS

A. Intrinsic Spectral Broadening

The relative Doppler bandwidth invariance theorem, presented in (2), was experimentally verified, in the present study, using a fully developed steady laminar flow model and porcine red cell suspensions at hematocrits between 2 and 40% as ultrasonic scatterers. Fig. 2 shows results obtained at a mean velocity of 30 cm/s. Fig. 2(a) presents examples of mean Doppler spectra for hematocrits of 4, 13, 29, and 41%, while Fig. 2(b) shows the relative bandwidth evaluated with (5), as a function of the hematocrit. Each data point in Fig. 2(b) corresponds to the average of 5 experiments performed on different days with different blood samples. The mean relative Doppler bandwidth for all hematocrit values was  $45.6 \pm 2.4\%$  ( $N = 65$ ). No statistical variation of the relative bandwidths was measured as a function of hematocrit ( $p = 0.97$ ). The averaged relative bandwidth attributed to the lack of resolution of the spectral algorithm (400 Hz / the averaged Doppler mean frequency) was approximately 9.5% for all measurements.

The effect of mean velocity variations on the relative Doppler bandwidths is presented in Fig. 3 for hematocrit values of approximately 40%. Fig. 3(a) shows examples of mean Doppler spectra at steady flow velocities of 10, 25, 40, and 55 cm/s. As seen, the bandwidth increases as the flow velocity increases. However, results in Fig. 3(b) show that the relative Doppler bandwidth is not significantly affected ( $p = 0.42$ ) by a variation in mean flow velocity. The mean value of the relative Doppler bandwidth from Fig. 3(b) is  $51.0 \pm 6.0\%$  ( $N = 20$ ). The averaged relative bandwidths due to the lack of resolution of the spectrum analyzer were 22.6, 10.9, 7.4, and 5.6% for mean flow velocities of 10, 25, 40, and 55 cm/s, respectively.

B. Nonstationary Spectral Broadening in Pulsatile Laminar Flow

The relative Doppler bandwidths were evaluated using Hanning data windows of 2.5, 5, and 10 ms. Results are

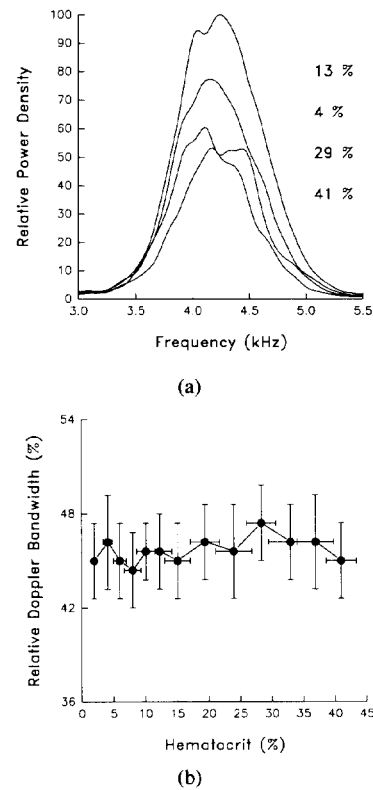
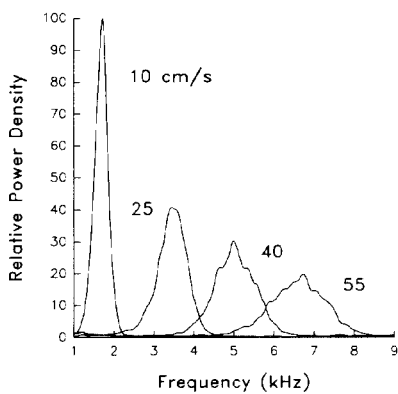


Fig. 2. (a) Typical mean Doppler spectra under steady laminar flow for a mean velocity of 30 cm/s and hematocrits of 4, 13, 29, and 41%. (b) The relative Doppler bandwidth (5) as a function of the hematocrit concentration. Each data point was averaged over five experiments. The mean spectra were averaged over 500 spectra and Hanning windows of 10 ms were used.

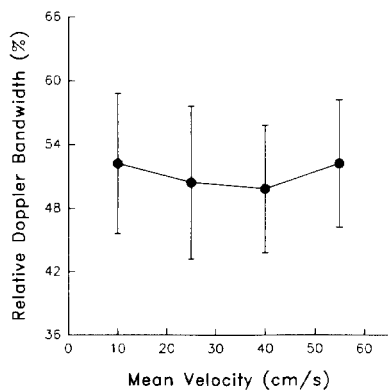
presented in Fig. 4 for pulsatile laminar flow experiments. A variation of the relative bandwidth was measured within the flow cycle for all data windows selected ( $p < 0.0001$ ). During flow acceleration, the relative bandwidth dropped while an increase was measured during flow deceleration. The smallest bandwidth was obtained slightly before peak systole. When comparing results for windows of 2.5, 5, and 10 ms, it can be observed from Fig. 4 that the relative Doppler bandwidth increases as the data window duration is decreased for both flow acceleration and deceleration intervals. Fig. 5 provides a comparison between the experimental measurement of the relative Doppler bandwidths based on (5) and the relative bandwidth attributed to the lack of resolution of the spectrum analyzer for Hanning data windows of 2.5 and 10 ms.

C. Doppler Spectral Skewness in Pulsatile Laminar Flow

The coefficients of skewness of Doppler mean spectra were evaluated within the flow cycle for window durations of 2.5, 5, and 10 ms. However, changing the window duration had no visible effect on the coefficients of skewness. Consequently, only results for windows of 10 ms are presented in Fig. 6. Positive skewness were obtained during flow acceleration while negative values were measured during flow deceleration. Just after peak systole, Doppler mean spectra had a symmetric shape. The one-way analysis of variance confirmed the significant variation of the coefficients of skewness within the flow cycle ( $p < 0.0001$ ). Fig. 7 shows examples of mean



(a)



(b)

Fig. 3. (a) Typical mean Doppler spectra under steady laminar flow, hematocrit of approximately 40%, and mean velocities of 10, 25, 40, and 55 cm/s, respectively. (b) The relative Doppler bandwidth (5) as a function of the mean flow velocity. Each data point was averaged over five experiments. The mean spectra were averaged over 500 spectra and Hanning windows of 10 ms were used.

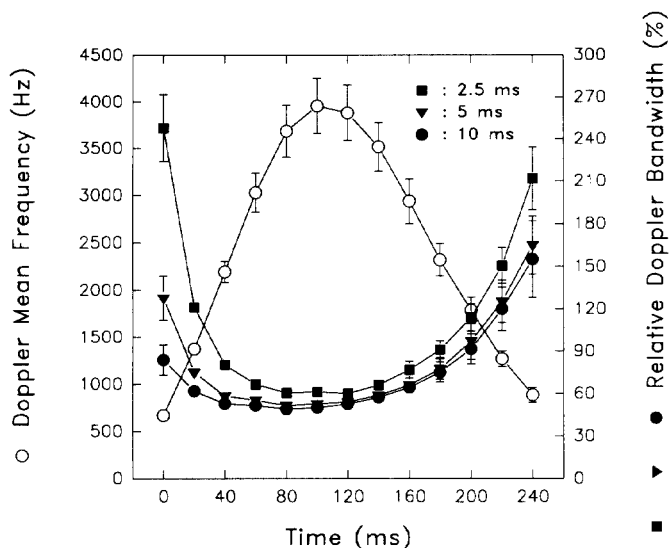
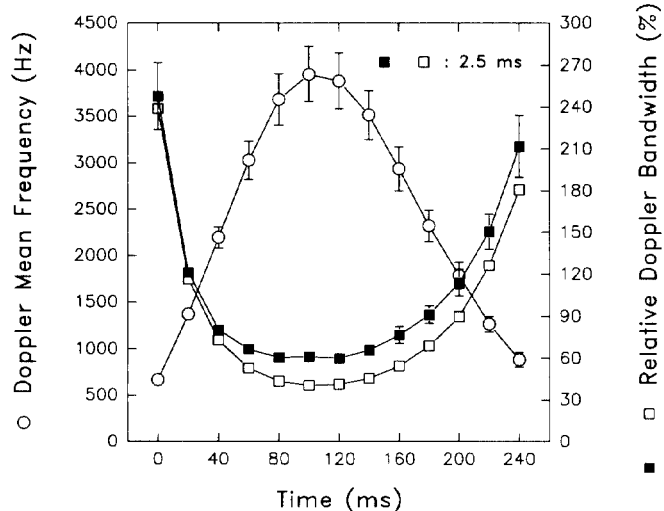
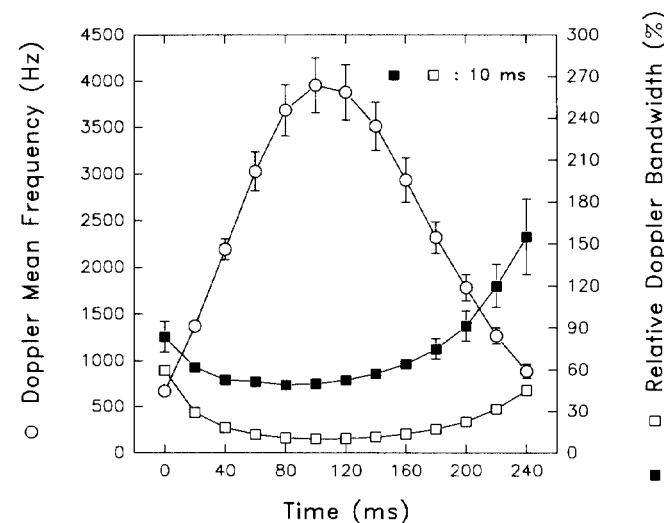


Fig. 4. Doppler mean frequency shift obtained from red cells moving within the sample volume under the pulsatile laminar flow, and relative Doppler bandwidth (5) as a function of the timing within flow acceleration and deceleration. Results are presented for Hanning data windows of 2.5, 5, and 10 ms. Each data point was averaged over five experiments and mean spectra were averaged over 200 cycles.

spectra during flow acceleration and deceleration, and the corresponding values of their coefficients of skewness  $\alpha_3$ .



(a)



(b)

Fig. 5. Doppler mean frequency shift obtained from red cells moving within the sample volume under the pulsatile laminar flow, and relative Doppler bandwidth as a function of the timing within flow acceleration and deceleration. The filled squares correspond to the experimental measurements of the relative bandwidth (5) while the hollow squares represent the relative bandwidth attributed to the lack of resolution of the spectral algorithm. Each data point was averaged over five experiments and mean spectra were averaged over 200 cycles. (a) Results for Hanning data windows of 2.5 ms. (b) Results for Hanning data windows of 10 ms.

#### D. Relative Doppler Bandwidth and Spectral Skewness in Pulsatile Turbulent Flow

The relative Doppler bandwidth and the coefficient of skewness were computed for each mean spectrum corresponding to the pulsatile turbulent flow situation using a Hanning window of 10 ms. Fig. 8(a) gives the variation of the relative Doppler bandwidth as a function of the timing within the flow cycle ( $p < 0.0001$ ). As the flow accelerated and then decelerated within the tube, the relative Doppler bandwidth increased almost linearly with a slope of 0.22%/ms ( $y = 0.22x + 18.08$ , correlation = 89.6%).

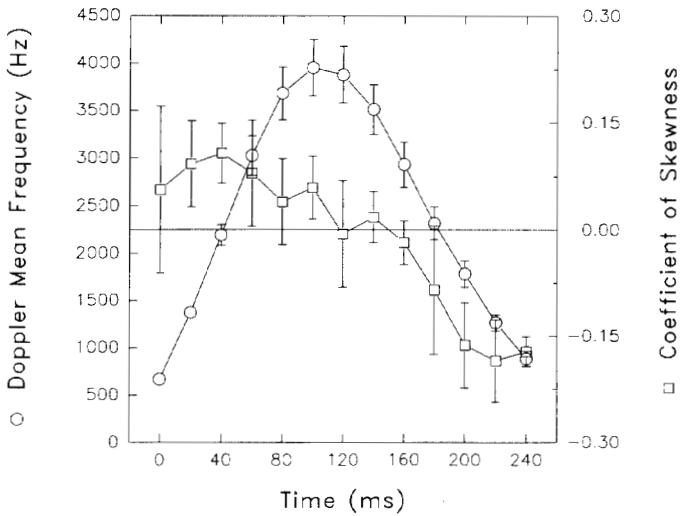


Fig. 6. Doppler mean frequency shift obtained from red cells moving within the sample volume under the pulsatile laminar flow, and coefficients of skewness of Doppler spectra (6) as a function of the timing within flow acceleration and deceleration. Each data point was averaged over five experiments. The mean spectra were averaged over 200 cycles and Hanning windows of 10 ms were used. The horizontal line in the graph represents the boundary between positively and negatively skewed spectra.

Fig. 8(b) shows the variation of the coefficients of skewness within the flow cycle ( $p < 0.0001$ ) for turbulent flow. For all moments of the flow cycle, the spectra were positively skewed. The maximal values of the coefficient of skewness were measured toward the end of flow deceleration. Fig. 9 presents an example of a mean spectrum with a coefficient of skewness of 0.90 in turbulent flow.

#### IV. DISCUSSION

##### A. Intrinsic Spectral Broadening

The influence of hematocrit on the relative Doppler bandwidth was presented in Fig. 2. From Fig. 2(a) and (b), it was observed that the intrinsic spectral broadening was not affected by red cell concentration, and consequently by changes in the correlation among particles. In the study by Censor *et al.* [6], one of their postulate was that the particles producing the Doppler spectrum had to be uncorrelated. The present study demonstrates that the relative Doppler bandwidth invariance theorem is still valid for correlated red cells.

Statistically significant different mean relative Doppler bandwidths were obtained between Figs. 2 and 3 ( $p < 0.001$ ). However, it is clear from these figures that the relative bandwidth is independent of both hematocrit and blood velocity variations. In Fig. 2, the averaged relative bandwidth was 45.6% while it was 51.0% in Fig. 3. This difference may be attributed to slight variations in the experimental protocol between both types of experiments.

##### B. Nonstationary Spectral Broadening

The results of Fig. 4 demonstrated that the relative Doppler bandwidth invariance theorem does not hold for pulsatile flow.

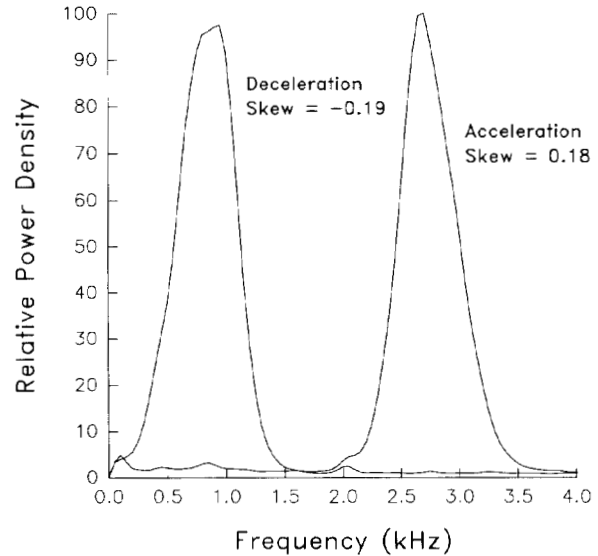
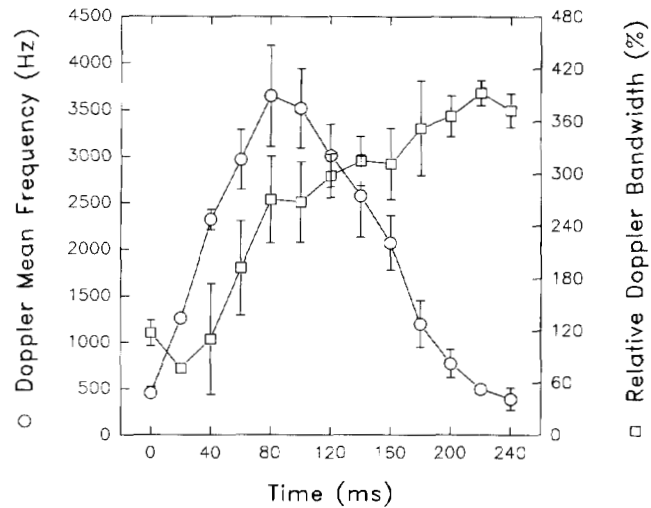


Fig. 7. Examples of Doppler mean spectra obtained during laminar flow acceleration and deceleration. The corresponding coefficients of skewness  $\alpha_3$  are also given. The mean spectra were averaged over 200 cycles and Hanning windows of 10 ms were used.

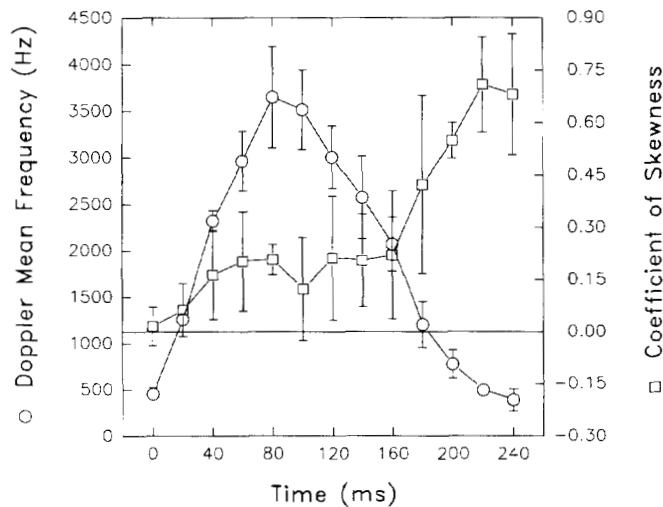
As reported in the Introduction, Kikkawa *et al.* [10] found that the backscattered Doppler signal is frequency modulated in nonstationary flow. The predicted higher bandwidth in pulsatile flow may also be attributed to another factor, namely the higher flow instability during flow acceleration and deceleration [16]–[18]. Shen [16] found that decelerating flows are generally less stable than accelerating flows. This observation seems to support our results since the largest relative bandwidths occurred toward the end of flow deceleration for Hanning windows of 5 and 10 ms.

The rationale behind the computation of the Doppler spectra using windows of 2.5, 5, and 10 ms was that smaller window duration should reduce the measured broadening due to the nonstationarity of the signal. As seen in Fig. 4, the opposite effect is observed. Reducing the length of the data window increases the measured relative Doppler bandwidth throughout the flow cycle. This effect is more severely apparent at the beginning of flow acceleration when the Doppler frequency shift is low. Two phenomena that influence the measured Doppler bandwidth have to be considered in pulsatile flow, namely the nonstationarity of the signal and the resolution of the spectral technique. From our results, it appears that the broadening due to spectral leakage dominates over that attributed to the nonstationarity of the signal for the smaller window, as shown in Fig. 5.

As reported previously, the frequency resolutions of the Fourier transform using Hanning windows of 2.5, 5, and 10 ms are 1600, 800, and 400 Hz, respectively. Since the broadening attributed to the spectral algorithm is independent of the flow velocity, the relative spectral broadening due to this effect should increase as the flow velocity is decreased. This is exactly what was observed in Fig. 5. The influence of a reduction of the data window was more apparent at the beginning of systole and at the end of flow deceleration when the flow velocity was low. The exact contribution of



(a)



(b)

Fig. 8. (a) Doppler mean frequency shift obtained from red cells moving within the sample volume under pulsatile turbulent flow, and relative Doppler bandwidth, and (b) coefficients of skewness as a function of the timing within flow acceleration and deceleration. Each data point was averaged over five experiments. The mean spectra were averaged over 200 cycles and Hanning windows of 10 ms were used. The horizontal line in (b) represents the boundary between positively and negatively skewed spectra.

nonstationary broadening and broadening associated with the spectral technique is difficult to estimate since both phenomena are probably not purely cumulative. However, we can certify from our results that both factors influenced the measured bandwidth since the relative bandwidth due to the limitation of the spectral algorithm (1600, 800, or 400 Hz divided by the mean frequency shift) was always lower than the experimentally measured bandwidths. The use of more appropriate spectral techniques, such as parametric modeling [19], [20] or time-frequency distribution algorithms [21], [22], would probably allow the reduction of both nonstationary broadening and broadening due to the limitation of the spectral technique.

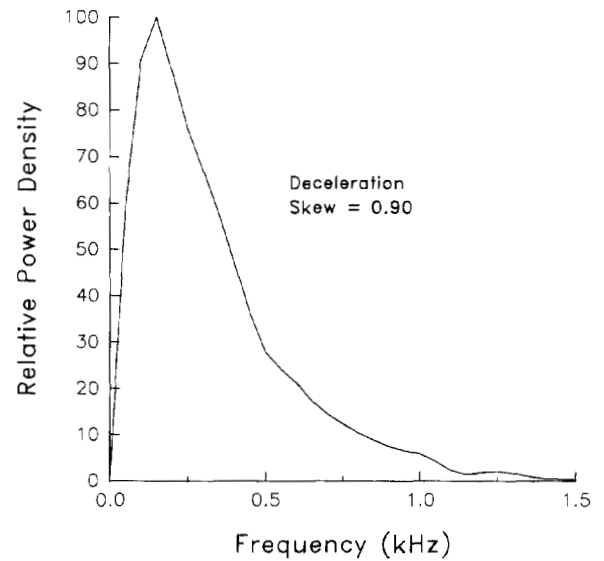


Fig. 9. Example of a mean Doppler spectrum obtained during turbulent flow deceleration. The corresponding coefficient of skewness  $\alpha_3$  (6) is also given. The mean spectrum was averaged over 200 cycles and a Hanning window of 10 ms was used.

For instance, parametric modeling does not necessitate the use of a long window duration to obtain a good resolution while time-frequency distribution provides instantaneous spectral computation.

### C. Skewness of Doppler Spectra

Little is known on the effect of pulsatile flow on the skewness of the spectral representation. Censor *et al.* [6] predicted changes in the skewness in unsteady flow while Kalman *et al.* [23] used this feature to detect carotid arterial occlusive disease. From our pulsatile laminar flow results, we observed positively skewed spectra during flow acceleration while negatively skewed spectra were found during flow deceleration. In pulsatile turbulent flow, the spectra were always positively skewed. It is believed that changes in the spatial location of red cells within the sample volume are responsible for the variation of the spectral skewness within the flow cycle.

### D. Relative Doppler Bandwidth in Pulsatile Turbulent Flow

The increase of the relative bandwidth observed in Fig. 8(a) during flow acceleration is clearly the result of an increase in turbulence intensity. For well-defined turbulent flow, turbulence intensity increases with the flow rate. The high spectral broadening during the deceleration phase may still be partially caused by turbulence created during acceleration since it takes time for the turbulence to subside in pulsatile flow. The combined effect of turbulence and flow instability, caused by the deceleration of blood, may explain the higher relative bandwidths during this phase of the flow cycle. As demonstrated by Ojha *et al.* [18], the deceleration of flow tends to increase turbulence intensity in constricted tubes. The same flow behavior was probably produced by the mesh screen used in our study.

### E. Comparison Between Theoretical and Experimental Results

In the present study, the bandwidths of Doppler spectra were obtained by computing the standard deviation of the spectral representations. In the experimental study by Tortoli *et al.* [9], the bandwidths at  $-3$ ,  $-6$ ,  $-10$ , and  $-20$  dB, below the dominant spectral peak, were used to verify the relative Doppler bandwidth invariance theorem. Depending on the signal-to-noise ratio of the signal, simple thresholding algorithms may fail in accurately detecting the boundary of the spectrum. In the theoretical derivation by Censor *et al.* [6], noise free spectra were considered. The minimal and maximal frequencies of the spectra were simply taken where the frequency components reached a power of zero. For noise free spectra, the relative Doppler bandwidth  $B_d/f_d$  is given by (2). For noise contaminated spectra, (5) provided a good estimate of the relative bandwidths.

The relative bandwidth computed from (2) can be estimated to compare our experimental results with the theoretical ones. In the present study, the diameter of the transducer was 0.3 cm ( $W$ ), the distance between the face of the transducer and the measurement site was 1.5 cm ( $F$ ), and  $\theta$  was  $60^\circ$ . Based on (2), the relative intrinsic Doppler bandwidth should be 35% which is smaller than the mean relative bandwidth of  $45.6 \pm 2.4\%$  shown in Fig. 2 and the mean value of  $51.0 \pm 6.6\%$  of Fig. 3. Several factors may be responsible for this difference between theoretical and experimental results. Error in the measurement of  $\theta$  and the presence of a parabolic flow profile may have contributed. As reported in the Section I, (2) is valid for a steady laminar flow characterized by a flat velocity profile (constant flow). In our experiments, a parabolic profile was present at the site of Doppler measurements which may explain the higher relative bandwidths measured.

The presence of unsteady flow may have also contributed to the difference between theoretical and experimental results. Several procedures, such as the use of a blood separator in the top reservoir [24], can be used to eliminate oscillations in the flow due to the roller pump. In our steady flow measurements [12], no such separator was used resulting in possible small oscillations at the site of Doppler measurements. Those oscillations may have also slightly contributed in increasing the relative bandwidth found in our study.

From the results of the pulsatile flow experiments shown in Fig. 4, the minimal relative bandwidth measured around peak systole was  $49.2 \pm 0.6\%$  for a data window of 10 ms. From (2), considering an angle  $\theta$  of  $70^\circ$ , the theoretical intrinsic spectral broadening (valid only for steady laminar flow) should be 55%. In pulsatile flow, the relative bandwidth cannot be smaller than the intrinsic broadening. The 5% difference between our experimental results and the theoretical derivation may also be attributed to the precision in the measurement of  $\theta$ . Precision errors in the measurement of  $W$  and  $F$  may have also contributed.

To evaluate the relative Doppler bandwidths  $B_d/f_d$ , it was hypothesized that the Doppler spectra had a shape matching that of a Gaussian distribution. For steady and pulsatile laminar flow experiments, this hypothesis was certainly justified but in pulsatile turbulent flow, the hypothesis may be invalid as

demonstrated in Fig. 9. Consequently, the relative Doppler bandwidths, indicated in Fig. 8, may have been overestimated toward the end of flow deceleration when the skewness became important. Instead of using a Gaussian model, a Poisson distribution would probably be better for those spectra.

### F. Clinical Implication

The results presented in the present study may have some clinical implications. Several spectral parameters were proposed in the literature to estimate the amount of spectral broadening and consequently the severity of arterial obstructions. The spectral broadening index, extracted from the maximal velocity spectrum (at peak systole), is one of these parameters that has extensively been used to quantify carotid arterial occlusive disease [23], [25]–[29]. From our results, by comparing Fig. 4 (data window of 10 ms) to Fig. 8(a), it can be observed that the difference between the relative bandwidths measure for laminar and turbulent flow increases during flow acceleration to reach a plateau around peak systole. Making measurements of the spectral broadening index at any moments between peak systole and the end of flow deceleration would probably provide similar results. However, as discussed previously, if nonstationary broadening could be minimized in laminar flow by using a better spectral algorithm than the Fourier transform, the extraction of the spectral broadening index at the end of flow declaration would probably be more sensitive to the severity of arterial disease.

The coefficient of skewness, computed in the present study, had also been used as a diagnostic parameter in an *in vitro* study by Kalman *et al.* [23]. Here again, the spectral parameter was extracted at peak systole. Figs. 6 and 8(b) show that a better performance would probably have been obtained using spectra computed toward the end of flow deceleration since the difference between the results for laminar versus turbulent flow is maximal over the period of the flow cycle.

## V. CONCLUSION

Results on an experimental evaluation of intrinsic spectral broadening, nonstationary broadening, and spectral skewness, using porcine red cell suspensions as ultrasonic scatterers, were presented. As discussed previously, the findings of the present study may have some clinical implications since information on the broadening of the Doppler spectrum has been used for many years to characterize blood flow abnormalities. In addition to the possible use of our results to improve the detection of arterial disease, the present study has also provided additional basic information on the backscattering of ultrasound from blood in both steady and pulsatile flow.

As mentioned in Section I, several factors contribute to the broadening of the Doppler spectrum. Unfortunately, the exact contribution of each of these factors on the measured spectrum is difficult to quantify in practice. When looking to a Doppler spectrogram obtained from a clinical instrument, all of these factors, namely intrinsic broadening, the velocity distribution within the sample volume, the flow characteristics, the nonstationarity of the signal, and the properties of the spectrum analyzer, contribute in distorting the spectrum. A

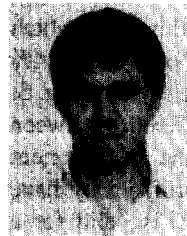
better knowledge of the effect of each of these factors may allow better instrument designs and better clinical use of the technique.

#### ACKNOWLEDGMENT

The authors gratefully acknowledge Mr. Louis Allard for revising the manuscript.

#### REFERENCES

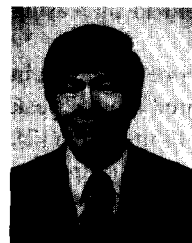
- [1] D. H. Evans, W. N. McDDicken, R. Skidmore, and J. P. Woodcock, *Doppler Ultrasound: Physics, Instrumentation, and Clinical Applications*. New York: Wiley, 1989 (reprinted in 1991).
- [2] V. L. Newhouse, P. J. Bendick, and L. W. Varner, "Analysis of transit time effects on Doppler flow measurement," *IEEE Trans. Biomed. Eng.*, vol. BME-23 pp. 381-387, Sept. 1976.
- [3] V. L. Newhouse, L. W. Varner, and P. J. Bendick, "Geometrical spectrum broadening in ultrasonic Doppler systems," *IEEE Trans. Biomed. Eng.*, vol. BME-24, pp. 478-480, Sept. 1977.
- [4] V. L. Newhouse, E. S. Furgason, G. F. Johnson, and D. A. Wolf, "The dependence of ultrasound Doppler bandwidth on beam geometry," *IEEE Trans. Sonics. Ultras.*, vol. SU-27, pp. 50-59, Mar. 1980.
- [5] P. A. J. Bascom, R. S. C. Cobbold, and B. H. M. Roelofs, "Influence of spectral broadening on continuous wave Doppler ultrasound spectra: A geometric approach," *Ultrasound Med. Biol.*, vol. 12, pp. 387-395, 1986.
- [6] D. Censor, V. L. Newhouse, T. Vontz, and H. V. Ortega, "Theory of ultrasound Doppler spectra velocimetry for arbitrary beam and flow configurations," *IEEE Trans. Biomed. Eng.* vol. BME-35, pp. 740-751, Sept. 1988.
- [7] K. K. Shung, R. A. Sigelmann, and J. M. Reid, "Scattering of ultrasound by blood," *IEEE Trans. Biomed. Eng.* vol. BME-23, pp. 460-467, Nov. 1976.
- [8] V. L. Newhouse and J. M. Reid, "Invariance of the transverse Doppler bandwidth with flow axis displacement," in *Proc. IEEE Ultrasonics Symp.*, Honolulu, HI, 1990, pp. 1533-1536.
- [9] P. Tortoli, G. Guidi, V. Mariotti, and V. L. Newhouse, "Experimental proof of Doppler bandwidth invariance," *IEEE Trans. Ultrason. Ferro. Freq. Control*, vol. 39, pp. 196-203; Mar. 1992.
- [10] S. Kikkawa, T. Yamaguchi, K. Tanishita, and M. Sugawara, "Spectral broadening in ultrasonic Doppler flowmeters due to unsteady flow," *IEEE Trans. Biomed. Eng.*, vol. BME-34, pp. 388-391; May 1987.
- [11] P. J. Fish, "Nonstationarity broadening in pulsed Doppler spectrum measurements," *Ultrasound Med. Biol.*, vol. 17, pp. 147-155, 1991.
- [12] K. K. Shung, G. Cloutier, and C. C. Lim, "The effects of hematocrit, shear rate, and turbulence on ultrasonic Doppler spectrum from blood," *IEEE Trans. Biomed. Eng.*, vol. 39, pp. 462-469, May 1992.
- [13] G. Cloutier and K. K. Shung, "Cyclic variation of the power of ultrasonic Doppler signals backscattered by polystyrene microspheres and porcine erythrocyte suspensions," *IEEE Trans. Biomed. Eng.*, vol. 40, Sept. 1993.
- [14] C. J. Hartley, *Reference Manual for 10 MHz Pulsed Doppler Flowmeter*. Houston, TX: Baylor College of Medicine, 1980.
- [15] J. S. Bendat and A. G. Piersol, *Engineering Applications of Correlation and Spectral Analysis*. Toronto, Canada: Wiley, 1980.
- [16] S. F. Shen, "Some considerations on the laminar stability of time-dependent basic flows," *J. Aerospace Sciences* vol. 28, pp. 397-404, 417, 1961.
- [17] J. H. Gerrard, "An experimental investigation of pulsating turbulent water flow in a tube," *J. Fluid Mech.*, vol. 46, pp. 43-64, 1971.
- [18] M. Ojha, R. S. C. Cobbold, K. W. Johnston, and R. L. Hummel, "Pulsatile flow through constricted tubes: an experimental investigation using photochromic tracer methods," *J. Fluid Mech.*, vol. 203, pp. 173-197, 1989.
- [19] S. L. Marple, Jr., *Digital Spectral Analysis with Applications*. Englewood Cliffs, NJ: Prentice-Hall, 1987.
- [20] Z. Guo, L.-G. Durand, L. Allard, G. Cloutier, H. C. Lee, and Y. E. Langlois, "Cardiac Doppler blood flow signal analysis. Part II: The time-frequency representation by using autoregressive modeling," *Med. Biol. Eng. Comput.*, vol. 31, pp. 242-248, May 1993.
- [21] F. Hlawatsch and G. F. Boudreaux-Bartels, "Linear and quadratic time-frequency signal representations," *IEEE Signal Process.*, pp. 21-67, Apr. 1992.
- [22] Z. Guo, L.-G. Durand, and H. C. Lee, "The time-frequency distributions of nonstationary signals based on a Bessel kernel," *IEEE Signal Process.*, vol. 40, pp. 3089, Dec. 1992.
- [23] P. G. Kalman, K. W. Johnston, P. Zuech, M. Kassam, and K. Poots, "In vitro comparison of alternative methods for quantifying the severity of Doppler spectral broadening for the diagnosis of carotid arterial occlusive disease," *Ultrasound Med. Biol.*, vol. 11, pp. 435-440, 1985.
- [24] Y. W. Yuan and K. K. Shung, "Echoicity of whole blood," *J. Ultrasound Med.* vol. 8, pp. 425-434, 1989.
- [25] M. S. Kassam, R. S. C. Cobbold, K. W. Johnston, and C. M. Graham, "Method for estimating the Doppler mean velocity waveform," *Ultrasound Med. Biol.* vol. 8, pp. 537-544, 1982.
- [26] P. M. Brown, K. W. Johnston, M. Kassam, and R. S. C. Cobbold, "A critical study of ultrasound Doppler spectral analysis for detecting carotid disease," *Ultrasound Med. Biol.*, vol. 8, pp. 515-523, 1982.
- [27] Y. Douville, K. W. Johnston, and M. Kassam, "Determination of the hemodynamic factors which influence the carotid Doppler spectral broadening," *Ultrasound Med. Biol.* vol. 11, pp. 417-423, 1985.
- [28] P. F. F. Wijn, P. van der Sar, T. H. J. M. Gootzen, M. H. J. Tilmans, and S. H. Skotnicki, "Value of the spectral broadening index in continuous wave Doppler measurements," *Med. Biol. Eng. Comput.* vol. 25, pp. 377-385, July 1987.
- [29] J. F. Morin, K. W. Johnson, and Y. F. Law, "Factors affecting the continuous wave Doppler spectrum for the diagnosis of carotid arterial disease," *Ultrasound Med. Biol.*, vol. 14, pp. 175-189, 1988.



**Guy Cloutier** (S'89-M'90) was born in Trois-Rivières, Québec, Canada in 1961. He received the B.Eng. degree in electrical engineering from the Université du Québec à Trois-Rivières in 1984, the M.S. and Ph.D. degrees in biomedical engineering from the École Polytechnique, Université de Montréal in 1986 and 1990, respectively.

Between 1990 and 1992, he was a postdoctoral research fellow of the Natural Sciences and Engineering Research Council of Canada at the Laboratory of Medical Ultrasonics, Bioengineering Program, Pennsylvania State University, University Park, PA. Since 1992, he has been a senior researcher at the Laboratory of Biomedical Engineering of the Institut de recherches cliniques de Montréal, and a research assistant professor at the faculty of medicine of the Université de Montréal. His research interests are in Doppler ultrasound and tissue characterization.

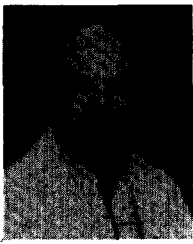
Dr. Cloutier is a member of the Quebec Engineer Association. He is also the recipient of a research scholarship (Junior I) from the Fonds de la Recherche en Santé du Québec



**K. Kirk Shung** (S'73-M'75-SM'89-F'93) was born in China in 1945. He received the B.S. degree in electrical engineering from the Cheng-Kung University, Taiwan in 1968, the M.S. degree in electrical engineering from the from the University of Missouri, Columbia, MO in 1970, and the Ph.D. degree in electrical engineering from the University of Washington, Seattle, WA in 1975.

Following a one-year postdoctoral training at Providence Medical Center, Seattle, he remained at that institution as a research bioengineer and held a joint appointment at the Institute of Applied Physiology and Medicine, Seattle, as a research scientist. Since 1979, he has been with the Bioengineering Program, Pennsylvania State University, University Park, PA, where he is now a professor. His research interests are in ultrasonic imaging and tissue characterization. He is the author of the textbook *Principles of Medical Engineering* (San Diego, CA: Academic Press, 1992) and the editor of *Ultrasonic Scattering in Biological Tissues* (New York: CRC Press, 1993).

Dr. Shung is a fellow of the American Institute of Ultrasound in Medicine and of the Acoustical Society of America. He is a founding fellow of the recently formed American Institute of Medical and Biological Engineering. He served on the NIH Diagnostic Radiology Section from 1985-1989 and is the recipient of the early career achievement award from the IEEE Engineering in Medicine and Biology Society in 1985.



**Louis-Gilles Durand** (M'78–SM'85) was born in St-Jean de Matha, Québec, Canada in 1949. He received the B.S., M.S., and Ph.D. degrees in electrical engineering from Ecole Polytechnique, University of Montreal, Montréal, Québec, Canada, in 1975, 1979, and 1983, respectively.

Since 1975, he has been with the Institut de recherches cliniques de Montréal as the Director of the Laboratory of Biomedical Engineering and more recently (1987) as the Director of the Department of Specialized Services. Since 1989, he is also a research associate professor in the Department of Medicine at the University of Montreal, an Adjunct Professor at the Institute of Biomedical Engineering of the Ecole Polytechnique, and since 1991, an Adjunct Professor at the Department of Electrical Engineering of McGill University, Montréal, Canada. His current interests are digital signal processing of the phonocardiogram and echo-Doppler signal, modeling of the heart–thorax acoustic system, and medical instrumentation.

Dr. Durand is a member of the Québec Order of Engineers, the American Heart Association, and the Canadian Medical and Biological Engineering Society.